Results in Materials 7 (2020) 100113

Contents lists available at ScienceDirect

Results in Materials

journal homepage: www.journals.elsevier.com/results-in-materials

Synthesis and characterization of graphene oxide from locally mined graphite flakes and its supercapacitor applications

Moses Kigozi [a,b,*], Richard K. Koech [a,d], Orisekeh Kingsley [a], Itohan Ojeaga [a], Emmanuel Tebandeke [c], Gabriel N Kasozi [c], Azikiwe P Onwualu [a]

[a] Department of Materials Science and Engineering, African University of Science and Technology, P.M.P 681, Abuja, Nigeria
[b] Department of Chemistry, Faculty of Science and Education, Busitema University, P.O BOX 236, Tororo, Uganda
[c] Department of Chemistry, College of Natural Science, Makerere University, P.O BOX 7062, Kampala, Uganda
[d] Department of Physics, Moi University, Kenya

ARTICLE INFO

Keywords:
Graphite flakes
Graphene oxide
Energy storage
Specific capacitance
Energy

ABSTRACT

Graphite is a mineral mined from different parts of the world which including Africa. It can be used or converted into different carbon materials such as exfoliated graphite, graphene, Graphene Oxide (GO), graphene nano platelets, carbon nano tubes, carbon onions among others by chemical or mechanical methods. The locally mined graphite flakes was converted to GO using chemical methods known as Hummer's oxidation method (HM). This method was also compared with other modified Hummer's methods by altering the conditions and the materials used. In the modified Hummer's method 1 (MHM1) a ratio of 9:1 of H_2SO_4/H_3PO_4 was used. While the modified Hummer's method 2 (MHM2) a reflux process was employed. The synthesized GO materials were characterized by different techniques such as UV–Vis spectroscopy, FTIR, SEM-EDX, XRD and electrochemical analysis. The morphology, functional groups, different bonds, elemental composition, crystallographic structure and energy storage applicability of the GO were examined. The techniques confirmed formation of functional groups like C–O, C═O and the C/O ratio in the materials. The electrochemical characterization performance of materials produced the highest specific capacitance of 211.2 F/g with a current density of 0.5 A/g and the specific energy of 7.33 Wh/kg.

1. Introduction

The science of design of nano materials involves different steps which include synthesis of the starting materials, characterization, optimisation, isolation exfoliation and cleaning. In the naturally occurring materials, carbon is the most abundant element in all organic substances on the universe. It occurs in many forms of different arrangements called allotropes of carbon with Africa as one of the continent with many mineral deposits like graphite among others. Its abundance makes it the main source of any form of carbon which include carbon black, graphene oxide, graphene, nanotubes, carbon onions, graphite, diamond to mention but a few [1]. Graphene oxide (GO) is in the category of graphite which can be processed by oxidation and mechanical methods. The graphene and its oxidised state has gained a lot of interest by both industrial application and academic research in fixing the earth's challenges and demand of materials. This is because of their interesting different properties which include mechanical, electrical among others [2,3]. Different raw materials are used in the process of synthesis of graphene oxide. Particulary, graphite flakes deposits which are present in Africa can be used as raw materials for the manufacture of materials such as Graphene oxide and other carbon materials like thermally expanded graphite used in fabrication for different application parts.

Graphene oxide (GO) can be synthesized chemically from graphite flakes. Graphene oxide in its structure contains different functional

Abbreviations: GO, Graphene Oxide; EC, Electrochemical; GCD, Galvanostatic Charge/Discharge; CV, Cyclic Voltammetry; EIS, Electrochemical Impedance Spectroscopy; HM, Hummer's method; MHM, modified Hummer's method; H2SO4, Sulphuric acid; NaNO3, Sodium nitrate; KMnO4, Potassium permanganate; H2O2, Hydrogen peroxide; HCl, Hydrochloric acid; UV–Vis, Ultra-Violet- Visible Spectroscopy; FTIR, Fourier Transform Infrared Spectroscopy; SEM, Scanning Electron Microscopy; EDX, Energy Dispersive X-ray; XRD, X-Ray Diffraction.

* Corresponding author. Department of Materials Science and Engineering, African University of Science and Technology, P.M.B 681, Abuja, Nigeria.
E-mail addresses: mkigozi@aust.edu.ng (M. Kigozi), rkoech@aust.edu.ng (R.K. Koech), korisekeh@aust.edu.ng (O. Kingsley), iojeaga@aust.edu.ng (I. Ojeaga), emmanuel.tebandeke@gmail.com (E. Tebandeke), gnkasozi@cns.mak.ac.ug (G.N. Kasozi), aonwualu@aust.edu.ng (A.P. Onwualu).

https://doi.org/10.1016/j.rinma.2020.100113
Received in revised form 10 June 2020; Accepted 11 June 2020
Available online 19 June 2020

groups attached on the basal planes and the sideways of the structure [4,5]. Graphene oxide has an sp^3 hybridized structure with layers of carbon. These are formed by the number of functional groups of oxygen [5,6] which makes it's hydrophilic with interlayers expansion [7]. GO also has ability to dissolve in a number organic solvents. This means it can be used in other materials like polymers and ceramics as a combination since it has high surface area. The high surface area makes GO a suitable material for energy storage devices for energy like batteries and super-capacitors [1]. The current research study focuses on the synthesis and characterization of GO from locally mined graphite flakes and its application for energy storage as supercapacitor electrode materials. The study presents conversion of graphite flakes into GO using Hummer's method (HM) and modified Hummer's method (MHM) which are chemical oxidation processes. This study was aimed at value addition of African raw materials for application.

The application of materials for energy storage is through their assessment to solve the challenges faced by manufacturing industries. The graphite flakes were converted into graphene oxide for application in energy storage as electrode materials for supercapacitors also known as Electric Double-layer Capacitors (EDLC). These are able to store energy and power to be delivered. The EDLC has high capacity of producing high power compared to batteries with a mechanism of charge transfer through the structure of the material using electrolyte and a separator between the electrodes [8,9]. EDLC have low weight, high cycle life, high power, low maintenance and work at a different thermal range from as low as −40 °C to as high as 70 °C without affecting its efficiency and no fear for explosion [8]. These devices can be used in systems where short cycle load is needed more frequently, such as in electric motor vehicles, mechanical systems with motors, washing machines, electric trains among others [10,11].

The performance of those materials greatly depends on electrical properties, surface area, pore volume, stability, interaction with the electrolyte among other [12,13]. GO is among the materials with different functional groups like COOH, CO, COC, OH which can enhance the performance of the EDLC devices [13–15]. GO is one of the carbon materials which has tremendous properties when it comes to application for energy storage [10,16] with high stability and light weight [10,17,18]. This gives high performance in capacitive application of EDLC and other hybrid types [19–24]. The EDLC stores its charge with non-faradaic or by electrostatic process where there is no charge transfer between electrolyte and electrode materials [25]. When the device is biased, the charge just accumulate at the surface of the electrode which causes charge attraction due to the potential difference resulting in diffusion of the electrolyte ions to go through the separator pores to another electrode enhance high power density [8].

In this respect, GO has gained substantial research interest in the field of energy storage for application in supercapacitors, batteries and hybrids, espcially due to their superlative properties. The recent advancement in the use of graphene oxide for supercapacitors as symmetric and asymmetric devices has attracted a lot of attention. This makes them lead the next generation device for energy storage although there is still a challenge of low performance for energy density and storage capacity [26,27].

There is great improvement in the performance of GO in asymmetric devices. Recently it has been reported that amorphous MoS_2 with reduced GO upon introduction of more sulphur sites increases the interaction of hydrogen ion from the electrolyte solution which increases the electrical conductivity, higher mechanical strength and surface area of the system. These properties help to increase the performance storage capacity of the materials up to a specific capacitance of 460 F/g at a current density of 1 A/g [26]. Also it has been reported that decollated nanostructure of conductive skeletons of carbon materials with binary transition metal sulphides improve the specific capacitance. Tao Liu et al., 2019 [28], reported FeNiS/rGO with a promising high performance specific capacitance of 2484 F/g at 1 A/g.

Focusing on the effective performance of the supercapacitors without losing their power density and stability, a number of metal oxide materials have been explored for high capacitance and high performance. This is due to their exceptional mesoporous structure and surface area. A number of non-noble metal oxide are used because they are environmental friendly and inexpensive and these include Fe_2O_3, MnO_2, NiO among others. Xiulun Sun et al., 2020 [27] synthesized α-Fe_2O_3 nanowires on a nickel form with $MgCl_2$ metal salt. The material exhibited an excellent electrochemical performance with specific capacitance of 1.57 F/cm^2 with current density of 1 mA/cm^2 with 98% specific capacitance retention [27].

2. Materials and methods

2.1. Chemicals and materials

Graphite flakes were utilized as locally supplied, sulphuric acid (98%), sodium nitrate (98%), Potassium permanganate (99%), Hydrogen peroxide (30%), and hydrochloric acid (35%) as supplied by Aldrich Sigma.

2.2. Conversion by oxidation of graphite flakes into graphene oxide (GO)

In the synthesis of GO from graphite flakes, Hummer's method (HM) and two modified versions of the Hummer's Methods (MHM) were used.

2.2.1. Hummer's method (HM)

GO was synthesized through oxidation process as that begun by addition of graphite flakes (2.0g) into $NaNO_3$ (2.0g) in a 500 ml beaker. 50 ml of concentrated H_2SO_4 was then added to the beaker under ice bath with continuous stirring for 2 h. After that time, 6.0 g of $KMnO_4$ was added carefully to the resultant mixture at a slow rate to control the temperature to be below 15 °C. The mixture was removed from the ice bath and put on a hot plate with magnetic stirrer at 35 °C and stirred for 2 days until pasty brownish colour formed. After 2 days, the mixture was slowly diluted with 100 ml of distilled water and the reaction temperature was increased rapidly to 98 °C causing effervescence and the colour change to brown [2]. The mixture was further diluted by addition of 200 ml of distilled water with continuous stirring. The dilute solution was finally treated with 10 ml of hydrogen peroxide to stop the reaction which changed to yellow solution with suspension. The sample was cleaned by rinsing and centrifuging with 10% HCl then followed with Deionised water for several rounds. The sample was then filtered and finally dried in a vacuum at 40 °C to obtain the GO powder.

2.2.2. Modified Hummer's method one (MHM 1)

The GO was synthesized from graphite flakes using modified conditions from Hummer's method [29]. Briefly, 2.0 g of graphite flakes was added to H_2SO_4/H_3PO_4 solution prepared by a volume ratio of 9:1 (180:20 ml). This was done under continuous stirring in the ice bath for 2 h. Then 7.3 g of $KMnO_4$ was slowly added to the mixture while keeping the temperature below 10 °C under continuous stirring for 2 days. After 2 days, 90 ml of distilled water was slowly added to the mixture with rapid mixing and the mixture turned dark brown with suspensions. This was further treated with 7.0 ml of H_2O_2 and 55 ml of distilled water for conversion of MnO_2 and residual permanganate into soluble $MnSO_4$. The mixture turned yellow colour with suspensions. The sample was cleaned 4 times with 150 ml of 3% warm HCl and DI water until pH 7.0 then filtered and dried under vacuum at 40 °C for 18 h.

2.2.3. Modified Hummer's method two (MHM 2)

Under this set up, Another method of synthesis for the GO from graphite flakes [2] was used. Briefly, 2.0 g of graphite flakes and 2.0 g of $NaNO_3$ were put in 1000 ml round bottomed flask and mixed with 90 ml of concentrated H_2SO_4 under ice bath with constant stirring for 4 h. After that time, 12.0 g of $KMnO_4$ was slowly added with controlled temperature below 10 °C. 184 mls of distilled water was added to the mixture at

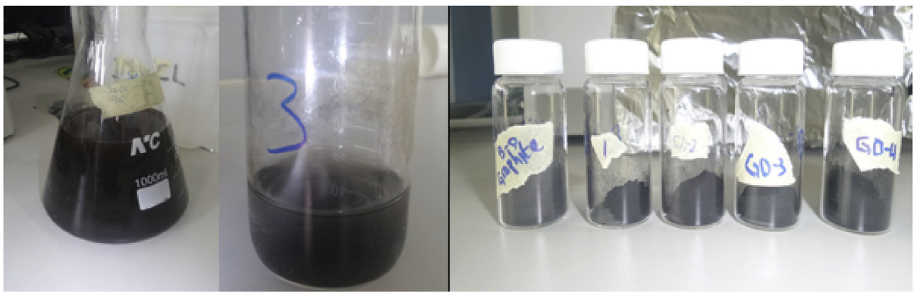

Fig. 1. Images of sample preparation.

constant stirring and the temperature was raised to 35 °C and kept at vigorous stirring for 4 h. The mixture was then refluxed at 98 °C for 10 min, the temperature was changed to 30 °C for 10 min, the solution turned brown colour, then the temperature changed to 25 °C and maintained at that temperature for 2 h. The solution was treated with 40.0 mls of H_2O_2 which terminated the reaction and changed the solution to a bright yellow colour. 400 ml of distilled water was added to the solution and stirred for 1 h then left to settle for 4 h, decanted off and filtered. The resultant suspension was cleaned repeatedly with 10% HCl and distilled water under centrifugation until neutral. This was dried at 60 °C for 8 h to get GO powder. The synthesis and preparation of GO are shown in Fig. 1.

2.3. Electrode preparation and electrochemical measurements

The synthesized GO from HM, MHM1 and MHM2 were prepared as active materials for electrodes in the construction of the EDLCs. The active materials were mixed with carbon black and PVDF as a binder in a ratio of 8:1:1 and NMP as a solvent for formation of the paste which was coated on the graphite foil with 1.0 cm^2 covered area. The coated electrodes were dried in an oven at 70 °C for 15 h. The mass of coated material was recorded after drying. The devices were assembled using Swagelok system to have a symmetric device with 6 M KOH as electrolyte.

The electrochemical analysis technique for testing the device was done on a BCS BIO-LOGIC 805 system with the two (2) electrode set up. Different testing techniques were carried out on the assembled devices to analyse their performance which included; cyclic voltammetry (CV), Galvanostatic charge-discharge (GCD), Electrochemical impedance Spectroscopy (EIS), Stability by voltage holding/floating and Self-discharge. The CV was carried out with the potential window of 1.0 V for different scan rates which included 5, 10, 20, 50, 70, 100, 200 and 500 mV/s. The GCD was performed with potential window range from 0 to 1.0 V using different current densities including 0.25, 0.5, 1.0, 1.5, and 2.0 A/g. The EIS was performed from high to low frequency range of 10 kHz to 10 MHz with the voltage of 10 mV. The voltage was varied from 10 mV to 20 mV to check on the behaviour of semi-circle and the curves at high frequency [30].

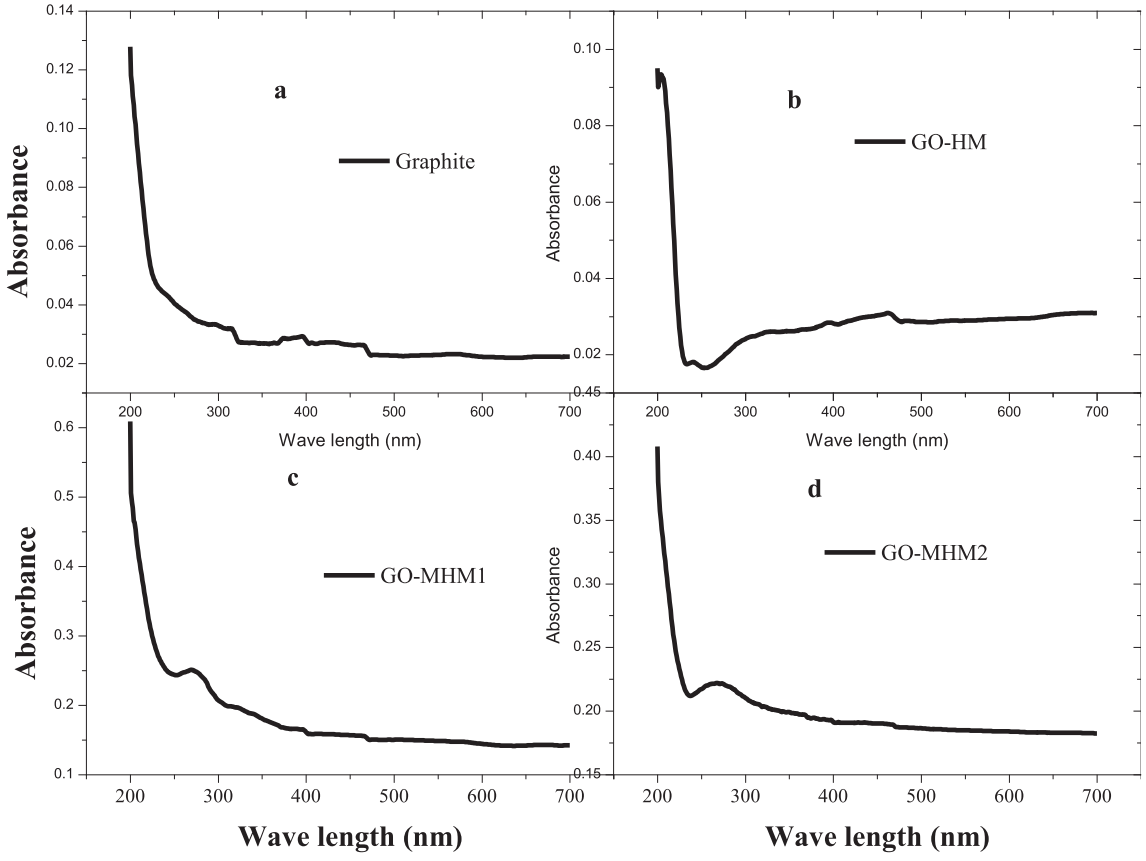

Fig. 2. UV–Vis spectra of Graphite and synthesized GO.

The stability test was performed by the technique of voltage holding or floating where the system sets 3 GCD cycles. Then at the 4th GCD charge cycle the voltage was kept at its maximum potential for 10 h s before performing another set of 3 GCD cycles. This was repeated until 130 h. The self-discharge was performed after stability study. This was carried out by charging the device to its maximum voltage using the 0.25 A/g current density. The charge was held at maximum for 5 min before being left to undergo self-discharge in the open circuit [30,31].

3. Results and discussions

3.1. Characterization of materials

The graphite flakes and GO synthesized by different methods were characterized by ultra-violet- visible spectroscopy (UV–Vis - D-50 SPECORD 50 PLUS Analytikjena German), Fourier transform infrared spectroscopy (FTIR - BRUKER Optics Model TENSOR 27 Germany), Scanning Electron microscopy (SEM - EVO LS 10 SEM modal) with Energy Dispersive X-ray (EDAX-AMETEK), X-Ray Diffraction (XRD - RIGUKU Smart-lab Auto sampler), Labram Micro Raman Spectrometer (Horiba Jobin Yvon model) and Electrochemical analysis techniques.

The UV-Vis absorption spectra of the samples are shown in Fig. 2. GO and graphite flakes samples were first dispersed differently in distilled water (0.5 mg/ml) and sonicated for 30 min to increase the dispersion in water [32]. The graphite flakes and GO samples were put in the cuvette and scanned between 200 and 700 nm wavelength as shown in Fig. 2. The absorption peaks in the spectra (Fig. 2) were observed at two different wavelengths. These two (2) specific kinds are feature characteristic that are used to identify GO from graphite flakes with one peak in the range of 320–360 nm as in Fig. 2a which appeared at wavelength of 310 nm. The first peak for GO that appears at around 230 nm wavelength is a corresponding identifier of a π-π* transition in aromatic C–C bond [33].

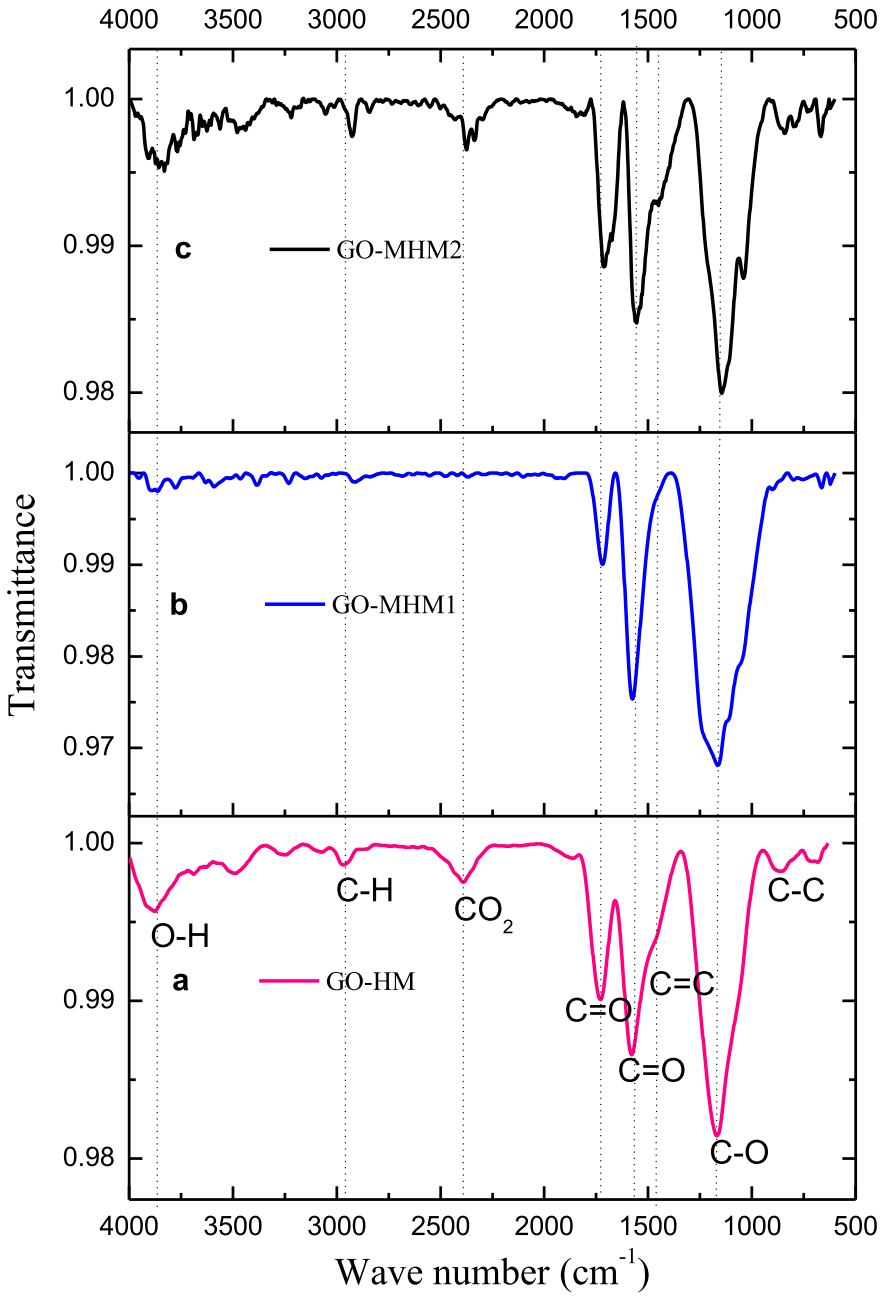

Fig. 3. FTIR spectra of GO synthesized with HM, MHM1 and MHM2 methods.

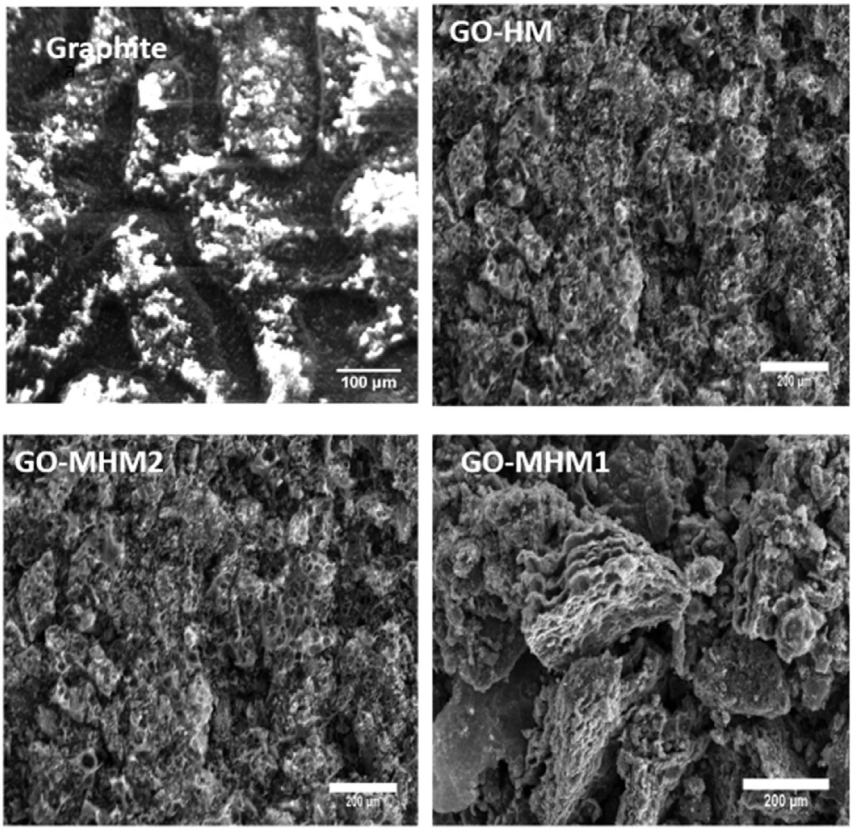

Fig. 4. SEM micrographs of Graphite and synthesized GO.

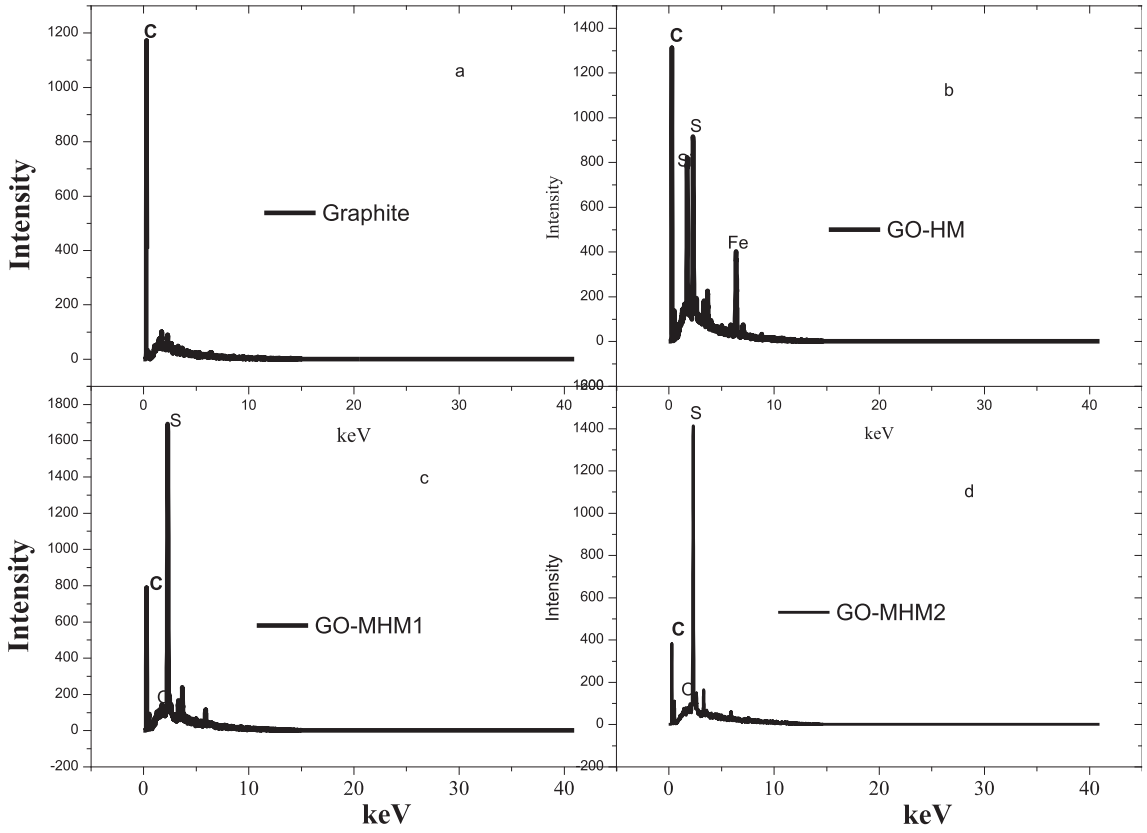

Fig. 5. *EDX spectra of Graphite and synthesized GO.*

Table 1
EDX elemental weight percentage of Graphite and synthesized GO.

sample	Elemental weight percentage											
	C	O	Si	S	Cl	K	Ca	Mn	Fe	Mo	Al	C/O
Graphite	95.47	0.3	1.02	–	–	–	–	–	–	3.09	0.11	318.2
GO-HM	44.59	2.08	6.09	9.78	1.38	2.02	3.78	–	30.29	–	–	21.4
GO-MHM2	48.2	2.41	–	30.24	1.12	2.55	6.18	9.31	–	–	–	20.0
GO-MHM1	56.02	6.73	–	29.09	3.35	4.8	–	–	–	–	–	8.3

The position and abundance of each sample peak slightly changed between the GO samples for the different methods as shown in Fig. 2b, c and 2d. The second peak shoulder which comes out at approximate range of 280 nm–300 nm corresponds to the identification of n-π^* transition of C═O bond [2,3,34].

To investigate the bond stretch interaction in the samples, FTIR spectrometer was used. Fig. 3 show different response at different wave number. In the fingerprint region (<1500 cm^{-1}) the sample materials depict the same peaks with characteristic stretches corresponding to C–C, C–O, C═C and C═O. The C–O showed the strongest peak followed by C═O at 1159 and 1576 cm^{-1} respectively. This is an of indication for oxidation of GO materials. The diagnostic region shown bonding at different wave number. The C═C stretching at 1461 cm^{-1} depicted in both GO-MHM2 and GO-HM, C═O stretching in all the GO samples at 1577 cm^{-1} and 1728 cm^{-1} (COOH group) [29,35–37]. GO-HM and GO-MHM2 samples shown a peak response at 2402 cm^{-1} which is an indication of a bond between GO and CO_2 which occurs at the temperature from 50 to 120 °C [38–40]. The C–H sp^3 stretching at 2770 cm^{-1} shown a weak response in the three (3) samples. The O–H/sp stretching was depict at 3876 with medium response with GO-HM and GO-MHM2 and weak response with GO-MHM1. The response of C═O bond confirms an existing bond before in oxidation process [41–44]. This shows absorptivity of GO for water molecules. The presence of hydrogen buckling bond orientation with carboxyl group tends to form a peak and valley with the edge interaction [45,46]. The presentation of the functional groups such as C═O and C–O in the GO materials further confirms that the graphite flakes were oxidised to GO [35,47,48].

The scanning Electron Microscopy (SEM) was employed to provide the structure and morphology of graphite flakes and GO [46]. Fig. 4a show the abundant carbon atoms on the surface of graphite flakes. Fig. 4(b c and d) show the particle morphology of the GO powder for the three (3) synthesized GO samples with their surfaces indicating the blend of carbon and oxygen [49]. EDX analysis depends on the atomic mass of elements in the samples for detection. The lower the atomic mass, the lower the response. The peak size depends on the abundance of the element in the sample. For graphite flakes and GO, the main element is carbon as shown by its largest peak. The EDX generates X-ray spectrum from the entire sample scanned areas using SEM images like in Fig. 4. Using the Noran System Six (NSS) software, the X-ray energy levels are associated with the individual elements in the sample and the orbital shell levels like K-shell that generated them.

The X-ray from the samples are generated by inelastic interaction of the beam of electrons with the sample atoms. These characteristic X-rays from the samples revealed as peaks imposed on the background of the continuum X-ray from the interaction of the electrons with the nucleus of the samples. The hole in K-shell of the sample atom of the samples is created by an incident high energy electron and then loses energy to the ejected electron.

The k-shell is then filled with an electron from the outer shell for the stability of the atom. The energy of the x-ray is related to the element atomic number from which the weight percentage is derived basing on the abundance of those atoms in the samples. From graph 1, the results show that the graphite flakes have a high number of C-atoms giving the weight percentage of 95.47% as in Table 1 and Fig. 5a. The concentration of oxygen is as low as 0.3% (Table 1 and Fig. 5a) which means there is likely no oxidation in the sample of graphite.

The Energy Dispersive X-ray analyser (EDX) spectra and elementally weight percentages were obtained for the graphite flakes and GO samples as shown in Fig. 5 (a, b, c & d) and Table 1. The x-rays from the samples are generated by inelastic interaction of the beam of electrons with the sample atoms. These characteristic x-rays from the samples are revealed as peaks (Fig. 5) imposed on the background of the continuum x-rays from the interaction of the electrons with the nucleus of the samples. The lower the atomic mass, the lower the response and the detector peak size depends on the abundance of the atoms of that element in the sample.

When graphite flakes were oxidised with Hummer's method (HM), the weight percentage of carbon decreased to 44.59% (Table 1) which created an increase in the atomic percentage by 2.08%. This shows that the method introduced more oxygen in the graphite to form graphene oxide. The process introduced other atoms like sulphur, potassium, chlorine, calcium and iron (Fig. 5b). This is possibly due to incomplete reactions and poor cleaning method of GO. These elements may have come from the initial chemicals and reagents used in the process of oxidation. With the MHM2 Fig. 5d indicated the oxidation response equal to HM as seen with C/O in Table 1 having the same ratio. The MHM 1 had an increased up to 6.73% with C/O ratio of 8 (Table 1). This means the method shown a better oxidation completion compared to the rest hence reducing the oxidising agent which in the removal of other elements like Manganese and Calcium (Table 1) showing the highest oxidation effect among all methods. In the process of oxidation, the reaction of Sulphur with carbon forming polysulphide hence reducing the interaction of oxygen with carbon [50].

This maybe so because the MHM1 uses high volume of concentrated acid combination than HM and MHM2 yet the weight of the graphite flakes remains the same in the both methods. This also be because of the ability for sulphur to accept a pair of electrons donated by another atom. Also when sulphur is in excess, can achieve a maximum covalence of six by expending to excited state forming SP^3d^2 hybrid orbitals which limits oxygen's interaction since it only forms homo-nuclear diatomic molecules. Also sulphur forms more oxides than its congeners.

The synthesized GO materials were analysed by X-Ray Diffraction (XRD) technique with a Cu kα source and JCPDS-ICDD library database

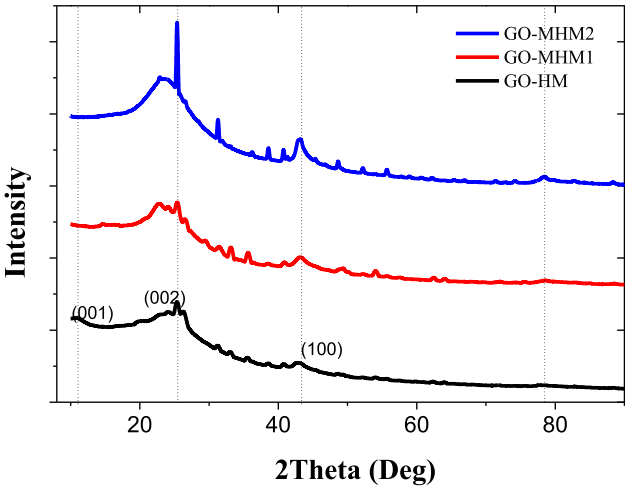

Fig. 6. XRD spectra for GO materials.

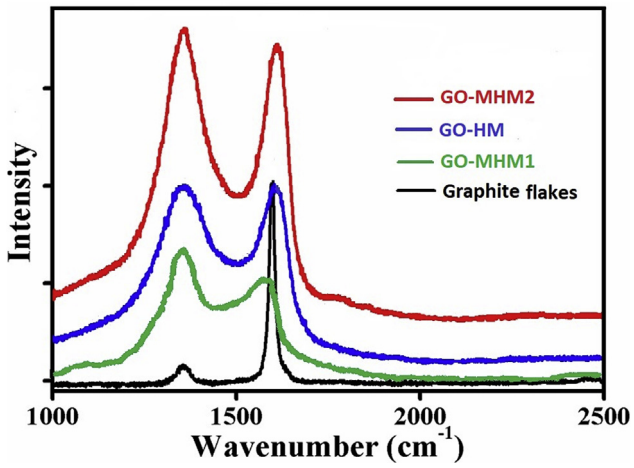

Fig. 7. Raman spectra for GO-HM, GO-MHM1, GO-MHM2 and graphite flakes.

to determine the materials average crystallite structural properties. Fig. 6 show the spectra of the GO materials indicating the formation of peaks at $2\Theta = 11^{\circ}$ with (001) plane, $2\Theta = 26.62^{\circ}$ with (002) plane and another peak at $2\Theta = 43^{\circ}$ with (100) plane which appeared in all the three (3) samples. The GO-MHM2 revealed another peak at $2\Theta = 77^{\circ}$ which is a reflection peak for graphitic nature of the material [35,36]. The peak at $2\Theta = 11^{\circ}$ indicate that there was oxidation of the graphite to form graphene oxide in all samples. The samples also shown other peaks at $2\Theta = 26.62^{\circ}$, 43° and 77° which indicates that the graphite was not completely oxidised to GO hence remaining in the samples [29,35–37].

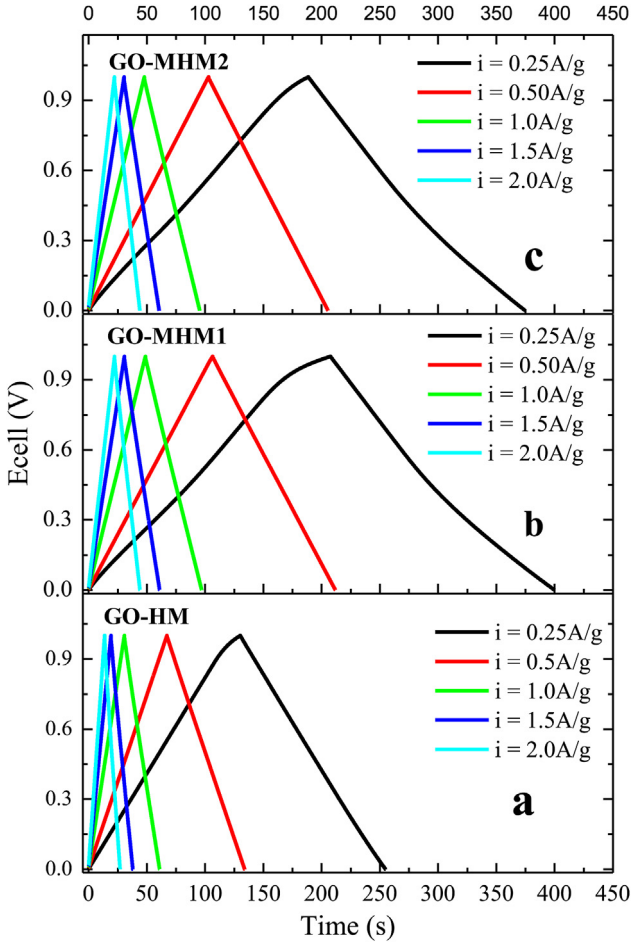

Fig. 8. Galvanostatic Charge/Discharge of GO materials prepared with HM, MHM1 and MHM2 methods using 6 M KOH as electrolyte at different current densities.

$$C = \frac{I\Delta t}{\Delta V} \tag{1}$$

The Raman spectroscopy was used to study the disorder and defects in the crystal structure. The disorder was determined by the intensity ratio between the disorder induced D band and the Raman allowed G band as I_D/I_G. As graphite flakes are oxidised into GO, the G band peak broadens and the D band intensity increases substantially indicating the decrease in the size of the in-plane sp^2 sites possibly due to the oxidation process. The D band for the materials appeared at approximately 1364 cm^{-1} and the G band at approximately 1600 cm^{-1} for GO-MHM2, GO-HM, GO-MHM1 and graphite flakes as shown in Fig. 7. The D band is as a result of reduction of the sp^2 domain size which introduces vacancies, defects and disorder due to oxidation process. The G band is due to the plane vibration which is very responsive with the sp^2 sites as a result of C–C bond stretch [51–53]. The I_D/I_G ratio for the materials was 1.25, 1.09.1.07 and 0.4 for GO-MHM1, GO-MHM2, GO-HM and graphite flakes respectively. The all the ratios are higher than that of graphite which indicate oxidation of the materials. GO-MHM1 shown the highest ratio indicating the higher oxidation process and this is in agreement with the EDX results where it showed the higher percentage of oxygen in the sample.

3.2. Electrochemical characterization of materials

The GCD curves of synthesized GO in 6 M KOH electrolyte is shown in Fig. 8 and Table 2. The specific capacitance (C_s) was calculated using equations (1) and (2). The capacitance (F) of the EDLC was evaluated using the discharge-time slope using equations [31,54,55].

The specific capacitance (F/g) for a single electrode using equation

$$C_s = \frac{2C}{0.5m_{el}} \tag{2}$$

where I is the applied current (A).

Δt is the discharge time (s)
ΔV is the change in potential (V)
M_{el} is the total mass of electrode material

The specific energy (E), specific power (P) and the efficiency (η) was also evaluated using the following equations [31,55,56];

$$E = \frac{CV_{max}^2}{2 \times 3.6m_{el}} \tag{3}$$

$$P = \frac{3600E}{\Delta t} \tag{4}$$

$$\eta_t = \frac{t_D}{t_C} \tag{5}$$

where t_D is the discharge time (s), t_C is the charge time (s) and V_{max} is the maximum potential (V).

From Fig. 8, the GO-MHM1 gave the highest specific capacitance (Cs) of 211.2 F/g at current density of 0.5 A/g as shown in Fig. 8b and Table 2. The trend of the specific capacitance for all GO materials were reducing with increased current density as shown in Table 2. The GO-MHM1 with C_s of 211.2 F/g gave specific energy of 7.33 Wh/kg as the highest with 250 W/kg of specific power and the efficiency of 99.15% (Table 2). GO-MHM2 in Fig. 8c with the C_s of 204.94 F/g at current density of 0.5 A/g as the highest for the material and the second highest among the three (3) GO materials. The C_s of 204.94 F/g shown specific energy of 7.12 Wh/kg and specific power of 250 W/kg and the efficiency of 99.45%. The GO

Table 2
The current density, specific capacitance (F/g), specific Energy (Wh/kg), specific Power (W/kg) and efficiency (%) of GO produced by HM, MHM1 and MHM2 using 6 M KOH electrolyte and potential of 1.0 V.

Sample	Current density (A/g)	Specific capacitance (C_s) (F/g)	Specific Energy (E) (Wh/kg)	Specific Power (P) (W/kg)	Efficiency (η) (%)
GO-HM	0.25	125.4	4.35	125	96.49
	0.5	133.16	4.62	250	98.72
	1	118.92	4.13	500	97.99
	1.5	112.5	3.91	750	97.81
	2	105.52	3.66	1000	95.30
GO-MHM1	0.25	192.49	6.68	125	92.74
	0.5	**211.2**	**7.33**	250	99.15
	1	195.4	6.78	500	100.95
	1.5	184.5	6.41	750	99.00
	2	176.72	6.14	1000	101.80
GO-MHM2	0.25	185.69	6.45	125	98.38
	0.5	204.94	7.12	250	99.45
	1	189.12	6.57	500	98.52
	1.5	183.48	6.37	750	99.93
	2	172.64	5.99	1000	97.12

synthesized by HM shown the lowest C_s performance with 133.16 F/g at current density of 0.5 A/g having the highest performance for GO-HM material. The C_s of 133.16 F/g shown specific energy of 4.62 Wh/kg and the specific power of 250 W/kg.

The C_s performance of the GO materials has a trend of GO-MHM1 > GO-MHM2 > GO-HM with the similar trend for the specific energy. This is because of the availability of oxygen functional groups on the surfaces of the material as depicted by EDX results in Table 1 with C/O ratio of 8.3 for GO-MHM1, 20.0 for GO-MHM2 and 21.4 for GO-HM. The oxygen functional groups heightens the performance of the EDLC [14,57]. The specific power of all the GO materials gave same performance with the same current density but increased with increased current densities with 2.0 A/g having the highest performance of 100 W/kg in all materials (Table 2). The efficiency of the devices were in the range of 92–101.8% which is the ideal performance of EDLC devices from porous carbon [55]. The C_s of the samples are higher than the GO [58] with measurement between 132 F/g in the scan rate range of 0.5–0.01 V/s and showing the highest specific energy of 6.74 Wh/kg and specific power of 190 W/kg from fabricated inkjet printed graphene electrodes. The reduced GO [38] has a C_s of 85 F/g at 1.0 A/g which is also lower than the current study. The results from the current work showed a lower performance compared to the reduced GO [10] with C_s of 430 F/g, specific energy of 8.96 Wh/kg and the specific power of 100.42 W/kg at the scan rate of 4 mV/s.

The Cyclic voltammogram (CV) of GO samples in the 6 M KOH electrolyte at the scan rate of 5, 10, 20, 50, 70, 100, 200 and 500 mV/s is shown in Fig. 8. The CV performance exhibited a symmetric and quasi-rectangular shapes in all the samples. This shape indicates the performance of high double layer capacitance (HDLC) [59,60].

This is indicative of EDLC capacitive behaviour and the shapes for all synthesized GO was maintained up to 500 mV/s (Fig. 9). From Fig. 9 (a and b), the shapes are similar with some small hump which indicate a little overcharging at high voltage [61]. Fig. 8c shows the best quasi-rectangular shape with no hump even 500 mV/s for the GO-MHM2.

The transport charge characterization of the electrode material was further performed by electrochemical impedance spectroscopy (EIS) technique. This was carried out in the frequency range of 10 kHz to 10 mHz in the open potential circuit using 6 M KOH as electrolyte. The Nyquist plot of the results are shown in Fig. 10. The potential was varied from 10 mV to 20 mV to determine the charge transfer resistance [61]. Fig. 10 shows the impedance plots with the similar behaviour in the high and low frequency regime. The plots from the material shown no semi-circles in frequency regime in the Nyquist plots (Fig. 10 insert). This indicates a good capacitance and high electrical conductivity of the GO electrode materials [38,57,62]. The EIS shows approximately the same resistance (0.82 Ω) for all the GO synthesized materials with the real frequency axis. This indicate a very low series resistance in the assembled devices which included electrolyte, current collector, surface of the materials and the Swagelok used in all the GO [13,54,61].

The Nyquist plot shows the vertical curves from the high frequency to the low frequency of the imaginary axis. This is an indication of low internal resistance and high conductivity [13]. The 45° and 90° angle line formation at high frequency regime in respect to the real axis of the impedance indicates the behaviours of the charge storage capacitive mechanism for the EDLC materials. From Fig. 10, when there are no semi-circles in the high frequency regime is a typical signature of

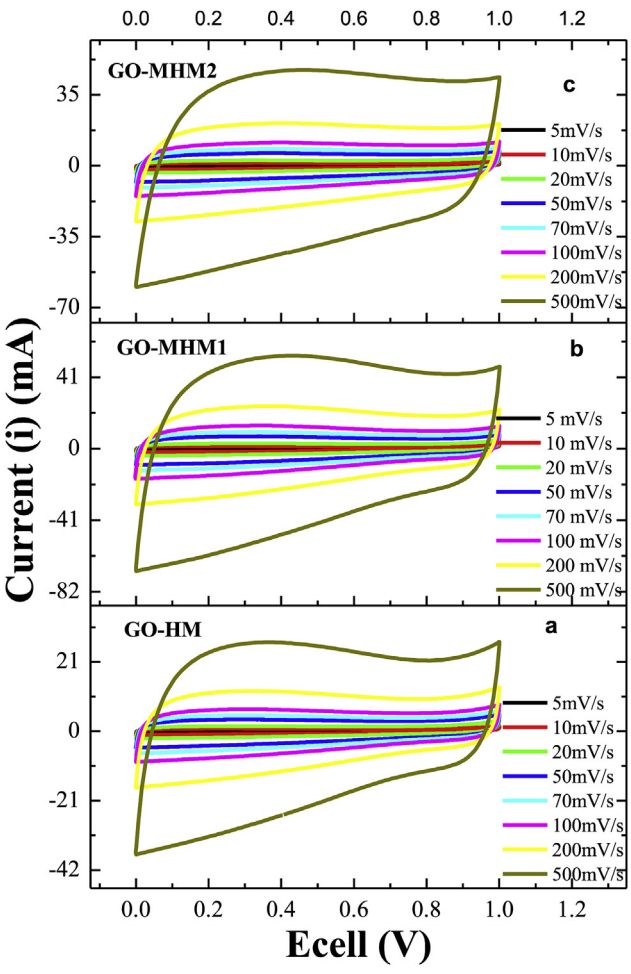

Fig. 9. Cyclic voltammetry of GO materials prepared with HM, MHM1 and MHM2 using 6 M KOH as electrolyte at different scan rates.

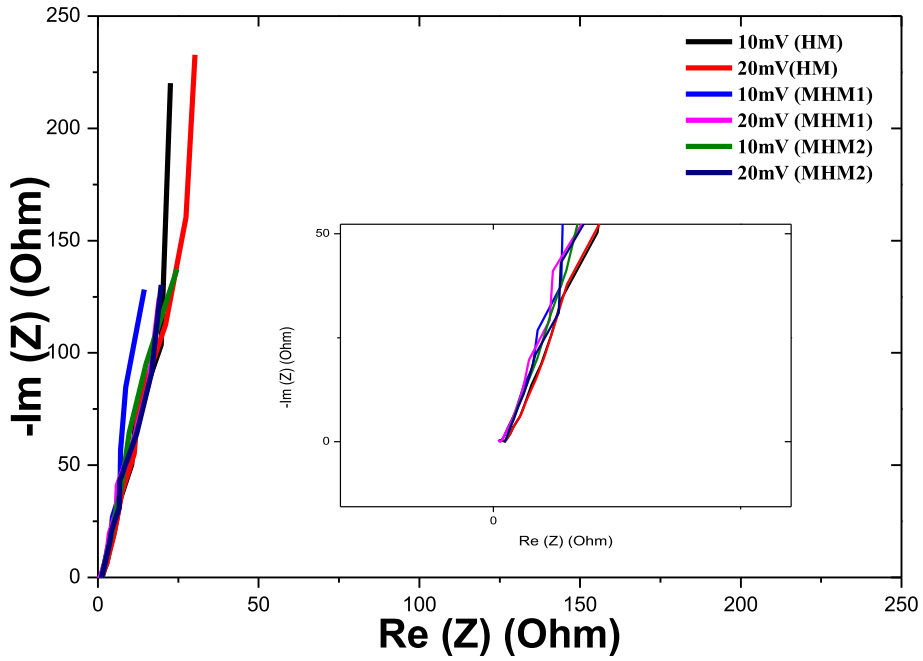

Fig. 10. Nyquist EIS plot for GO materials at different voltages for the three methods used.

supercapacitor materials. This is because porous carbon electrode materials stores its charge in the physical behaviour without any charge transfer in the process [61]. To validate if there is any formation of the semi-circle at high potential. The EIS was carried out at different potential and also to ascertain the charge transfer resistance. After performing the EIS at 10 and 20 mV, the curves shown no change at high frequency regime but only a small deviation at low frequency of the imaginary regime which indicates there was no charge transfer resistance but only small internal resistance causing a small deviation at the low frequency regime of the imaginary axis as shown in Fig. 10 and its insert.

The stability of the assembled devices was carried out by voltage holding/floating methods as indicated in Fig. 11 insert. Fig. 11 show the performance of the voltage holding for a duration of 130 h. This is a new conventional cycling method which has been found to be a more realistic and reliable way for stability testing of supercapacitors [30,31]. This method gives real stability tough conditions like holding charge at its maximum for 10 h before discharge cycle which causes degradation details which may occur in the electrochemical process of the device [30].

It can be seen from Fig. 11 that performance decrease in the specific

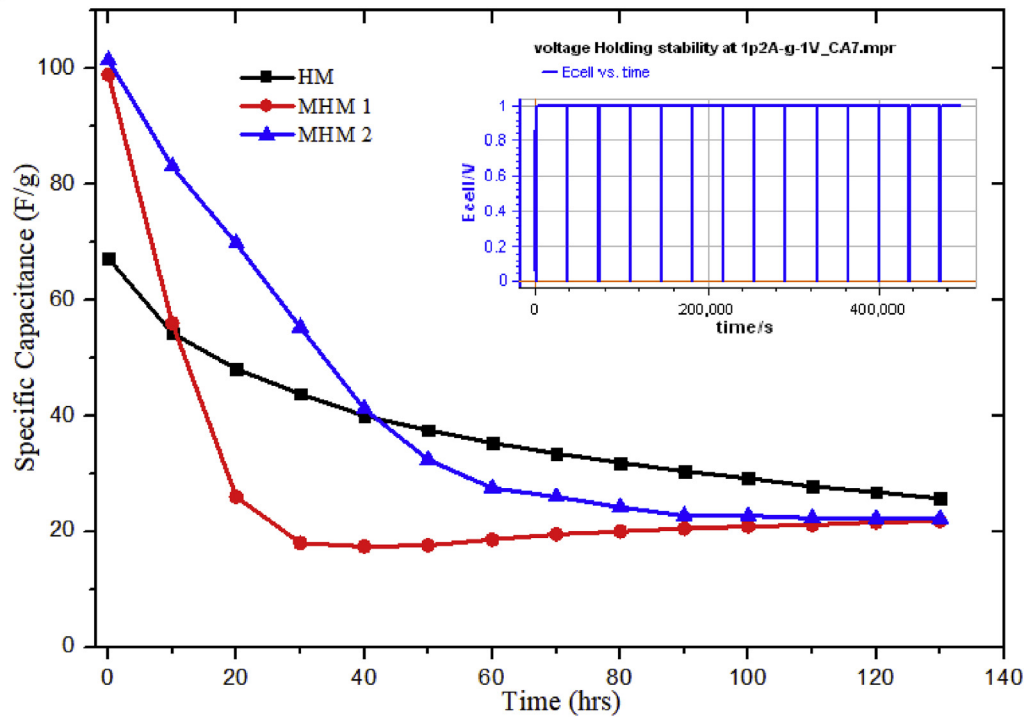

Fig. 11. Voltage holding stability of GO materials prepared with HM, MHM 1 and MHM 2 methods and EC stability display in the insert.

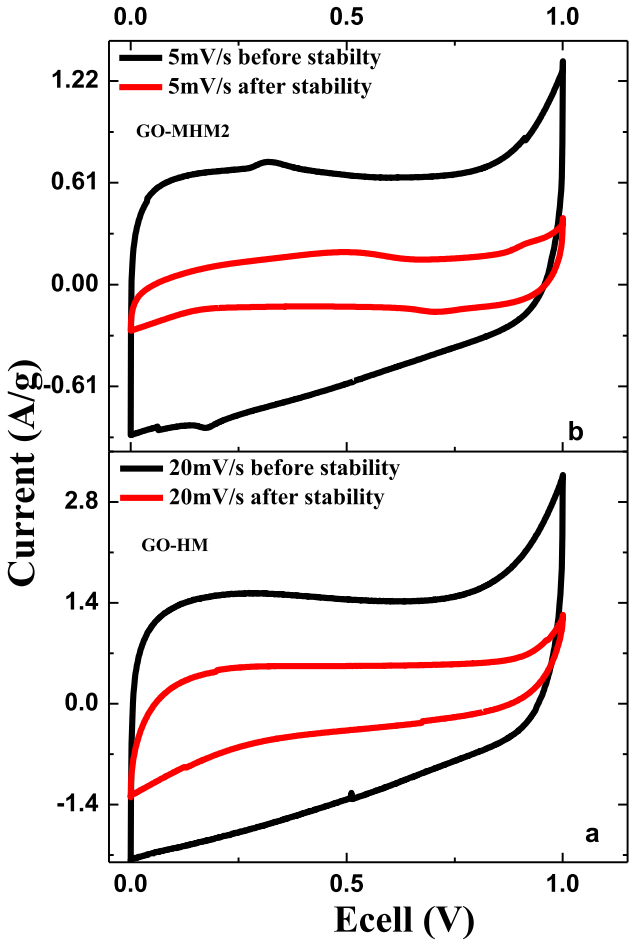

Fig. 12. CV for the GO materials before and after voltage holding stability test.

capacitance after 10 h and continued to decrease slowly until the end of 130 h. The GO-MHM2 and GO-HM shown 17% capacitance fade after 10 h and GO-MHM1 exhibited a 45% fade. The fading in GO-HM was more stable than other GO materials which kept a 50% loss at the end of 130 h. The loss of capacitance of GO-MHM2 stabilized at a loss of 70% after 70 h which further lowered to 80% at the end of 130 h. At the end 30 h, GO-MHM1 lost up to 80% and was kept at that level until 130 h. This indicates that there was high intercalation in the materials with electrolyte between 10 and 60 h which may be due to interaction of K^+ ions from the

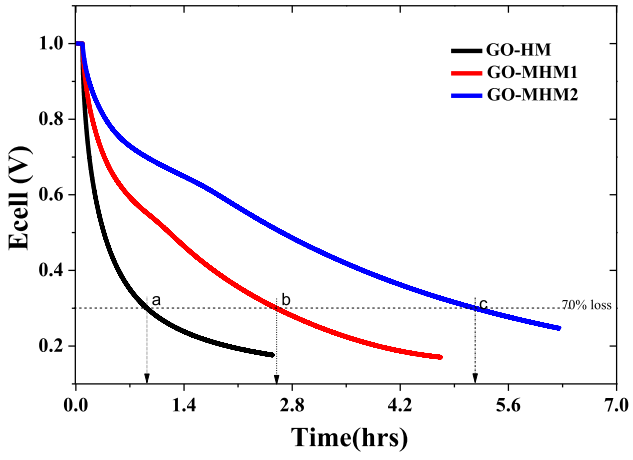

Fig. 13. Self-discharge of GO materials after charging the device to 1 V and holding for 5 min in an open circuit.

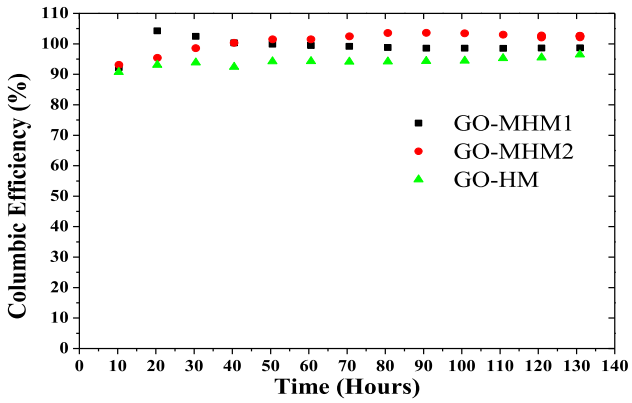

Fig. 14. The plot of columbic efficiency % versing stability voltage holding time in hours.

electrolyte at high potential. This may also be due to K^+ ion interaction with oxygen functional groups on the surface of the material causing faradaic reactions as shown in Fig. 12.

The faradaic reactions were revealed by the CVs carried out before and after stability as shown in Fig. 12. Fig. 12 show exponential peaks at high voltage which may be due to dissociation of the electrolyte and interaction of the K^+ ions with the surface of the materials. There is also reduction of the shape size in Fig. 12 after stability which implies there is a loss of capacitance due to these mentioned factors. The high capacitance fade in the current work is similar to that performed on YP17/PTFE [63] when comparing voltage holding testing method with conventional cycling where they obtained a capacitance loss of 68% within 100 h and 97% loss after 500 h with voltage holding method yet conventional cycling shown 2% after 50,000 cycles which took approximately 800 h.

In comparing voltage holding with conventional cycling [64], reported capacitance loss of 30% after 20 h with voltage holding at 3.5 V which required 300 h for conventional cycling to observe the same loss [64]. Concluded that voltage holding was more time efficient than cycling test. The fact is that during voltage holding, the capacitor is subjected constantly to maximum potential for a long holding time keeping the dissociated ions in contact with the materials yet in conventional cycling, the capacitor is only exposed to the mutable potential [31,64].

The self-discharge is another important technique for evaluation of the life of the supercapacitor. This was carried out after the voltage holding test on the same device. The devices were charged up to 1.0 V and hold for 5 min before they were left to self-discharge in an open circuit. Fig. 13 show the performance of the assembled devices from the GO synthesized materials. The GO-MHM2 shown voltage loss of 70% after 5.2 h (part c in Fig. 13) showing to be a better performer than the other materials. GO-MHM1 lost 70% in less than 2.8 h and GO-HM in less than 1.2 h as shown in Fig. 13-part b and part a respectively.

The columbic efficiency verses stability voltage holding time in hours shown in Fig. 14 for the three synthesized materials. The stability test was carried out by voltage holding/floating with three (3) charge-discharge before holding the voltage at maximum of 1.2 V for 10 h before another cycling round. equation (5) was used to evaluate the columbic efficiency of the material with the discharge/charge time for each second cycle from the 3 cycles. The GO-MHM2 shown the highest retention of 102% followed by GO-MHM1 with 99.1% and GO-HM with the lowest retention of 96.5% which was maintained after performing the test for 130 h.

4. Conclusion

The GO materials were synthesized successful from graphite flakes using hummer's method and two other modified methods from Hummers with a change in some conditions and materials used. The materials were

characterized with different techniques which included UV–Vis spectroscopy, FTIR, SEM-EDX, XRD and electrochemical analysis to the check their applicability for energy storage in supercapacitors. The characterization techniques confirmed the existence of different functional groups which are key in GO. These include C–O, C═O and main elements like carbon and oxygen. The presentation of the functional groups such as C═O and C–O in the GO materials further confirms that the graphite flakes were oxidised to GO. EC performance of the GO materials as supercapacitor electrode materials also confirmed the usefulness of the materials for EDLC device application.

Authors' contributions section

KM carried out the experimental design, synthesis, analysis, data interpretation and writing up of the manuscript. RKK participated in the draft of the manuscript and referencing of the work. OK carried out the UV–Vis analysis. IO participated in the experimental design and procurement of items needed. TE and KG participated in chemical data interpretation of the analysis results. PAO was the coordinator and supervisor of the whole work and proof reading of the work. The work was read and approved by all members for final manuscript.

Funding

This research did not receive any specific grant from funding agencies in the public, commercial, or not-for-profit sectors.

Declaration of competing interest

The authors declare that they have no known competing financial interests or personal relationships that could have appeared to influence the work reported in this paper "Synthesis and characterization of graphene oxide from locally mined graphite flakes and its supercapacitor applications".

Acknowledgement

The researchers that participated in the study were supported by Africa Centre of Excellence in materials, product Development and nanotechnology (MAPRONANO), Pan African Materials Institute (PAMI) and AfDB laboratory in African University of Science and Technology. Moses Kigozi acknowledges Dr PK Jain for all his support given during the study visit as a Visiting Scholar in ARCI. Authors thank ARCI under DST India for supporting this study through the research fellowship scheme.

References

[1] B. Paulchamy, G. Arthi, L. Bd, A simple approach to stepwise synthesis of graphene oxide nanomedicine & nanotechnology, J. Nanomed. Nanotechnol. 6 (1) (2015) 1–4, https://doi.org/10.4172/2157-7439.1000253.
[2] K.S.S.K. Muhamad, et al., Synthesis and characterization of exfoliated graphene oxide, AIP 1784 (2016), 040013–5.
[3] M.S. Eluyemi, M.A. Eleruja, A. V Adedeji, B. Olofinjana, O. Fasakin, O.O. Akinwunmi, Synthesis and characterization of graphene oxide and reduced graphene oxide thin films deposited by spray pyrolysis method, Graphene 5 (July) (2016) 143–154.
[4] W. Cai, et al., Synthesis and solid-state NMR structural characterization of 13C-labeled graphite oxide, Sci. AAAS 321 (1815) (2008).
[5] W. Gao, L.B. Alemany, L. Ci, Pulickel M. Ajayan, New insights into the structure and reduction of graphite oxide, Nat. Chem. (2009) 6.
[6] Q. Zheng, Z. Li, J. Yang, J. Kim, Graphene oxide-based transparent conductive films, Prog. Mater. Sci. 64 (2014) 200–247.
[7] C. Sekhar, C. Ray, Application and uses of Graphene oxide and Reduced graphene oxide, in: A Volume of Micro and Nano Technologies, 2015, pp. 39–55.
[8] Z.S. Iro, C. Subramani, S.S. Dash, A brief review on electrode materials for supercapacitor, Int. J. Electrochem. Sci. 11 (2016) 10628–10643, https://doi.org/10.20964/2016.12.50.
[9] M.A. Pope, S. Korkut, C. Punckt, I.A. Aksay, Supercapacitor electrodes produced through evaporative consolidation of graphene oxide-water-ionic liquid gels, J. Electrochem. Soc. 160 (10) (2013) A1653–A1660.
[10] Y. Chang, et al., Flexible supercapacitor electrode with high performance prepared from graphene oxide films assembled in the presence of p - phenylenediamine and urea, J. Mater. Sci. Mater. Electron. 30 (2019) 7216–7225, https://doi.org/10.1007/s10854-019-01000-0.
[11] A.K. Mittal, M.J. Kumar, Electrochemical double-layer capacitors featuring carbon nanotubes, Encycl. Nanosci. Nanotechnol. 13 (271) (2011) 263–271.
[12] B. Rajagopalan, J.S. Chung, Reduced chemically modified graphene oxide for supercapacitor electrode, Nanoscale Res. Lett. 9 (1) (2014) 1–10.
[13] L. Lai, et al., Preparation of supercapacitor electrodes through selection of graphene surface functionalities, ACS Catal. 6 (7) (2012) 5941–5951, https://doi.org/10.1021/nn3008096.
[14] H. Gomez, M.K. Ram, F. Alvi, P. Villalba, E. Stefanakos, A. Kumar, Graphene-conducting polymer nanocomposite as novel electrode for supercapacitors, J. Power Sources 196 (2011) 4102–4108.
[15] N.L. Yang, J. Zhai, M.X. Wan, D. Wang, L. Jiang, Layered nanostructures of polyaniline with graphene oxide as the dopant and template, Synth. Mater. 160 (2010) 1617–1622.
[16] X. Li, B. Wei, Supercapacitors based on nanostructured carbon, Nanomater. Energy 2 (2) (2013) 159–173.
[17] L. Dong, Z. Chen, S. Lin, K. Wang, C. Ma, H. Lu, reactivity-controlled preparation of ultralarge graphene oxide by chemical expansion of graphite, Chem. Mater. ACS 29 (2) (2017) 564–572.
[18] S. Zhang, Y. Yan, Y. Huo, Y. Yang, J. Feng, Y. Chen, Electrochemically reduced graphene oxide and its capacitance performance, Mater. Chem. Phys. 148 (3) (2014) 903–908.
[19] Y. Zhai, Y. Dou, D. Zhao, P.F. Fulvio, R.T. Mayes, S. Dai, Carbon materials for chemical capacitive energy storage, Adv. Mater. 23 (42) (2011) 4828–4850.
[20] T. Kuila, S. Bose, A.K. Mishra, P. Khanra, N.H. Kim, J.H. Lee, Chemical functionalization of graphene and its applications, Prog. Mater. Sci. 57 (7) (2012) 1061–1105.
[21] B. Lobato, V. Vretenar, P. Kotrusz, M. Hulman, T.A. Centeno, Reduced graphite oxide in supercapacitor electrodes, J. Colloid Interface Sci. 446 (2015) 203–207.
[22] S. Chen, et al., Scalable non-liquid-crystal spinning of locaaly aligned graphene fibers for high-performance wearable supercapacitors, Nanomater. Energy 15 (2015) 642–653.
[23] W. Ma, et al., Hierachical MnO2 nanowire/graphene hybrid fibers with excellent electrochemical performance for flexible solid-state supercapacitors, J. Power Sources 306 (2016) 481–488.
[24] K. Leng, et al., Graphene-based Li-ion hybrid supercapacitors with ultrahigh performance, Nano Res. 6 (8) (2013) 581–592.
[25] M.V. Kiamahalleh, S.H.S. Zein, G. Najafpour, S.A. Sata, S. Buniran, Multiwalled carbon nanotubes based nanocomposites for supercapacitors: a review of electrode materials, Nano 7 (2) (2012) 1230002.
[26] P. Hota, et al., Ultra-small amorphous MoS2 decorated reduced graphene oxide for supercapacitor application, J. Mater. Sci. Technol. 40 (2020) 196–203, https://doi.org/10.1016/j.jmst.2019.08.032.
[27] S. Xiulun, et al., One-dimensional Mg2+-induced α-Fe2O3 nanowires for high-performance supercapacitor, Results Mater. 5 (100052) (2020) 6, https://doi.org/10.1016/j.rinma.2019.100052.
[28] T. Liu, L. Li, L. Zhang, B. Cheng, W. You, J. Yu, 0D/2D (Fe0.5Ni0.5)S2/rGO nanocomposite with enhanced supercapacitor and lithium ion battery performance, J. Power Sources 426 (April) (2019) 266–274, https://doi.org/10.1016/j.jpowsour.2019.04.053.
[29] N.M.S. Hidayah, et al., "Comparison on graphite , graphene oxide and reduced graphene oxide: synthesis and characterization, in *Global Network for innovative Technology* (October) (2017), https://doi.org/10.1063/1.5005764.
[30] A. Bello, et al., Floating of PPY derived carbon based symmetric supercapacitor in alkaline electrolyte, E C S Soc. Electrochem. 75 (24) (2017) 1–12, https://doi.org/10.1149/07524.0001ecst.
[31] F. Barzegar, et al., Cycling and floating performance of symmetric supercapacitor derived from coconut shell biomass, AIP Adv. 6 (115306) (2016) 9, https://doi.org/10.1063/1.4967348.
[32] V. Nicolosi, M. Chhowalla, M.G. Kanatzidis, M.S. Strano, J.N. Cleman, Liquid Exfoliation of layered materials, Sci. AAAS 340 (2013) 1226419.
[33] T. Fentaw, D. Worku, "Controlled synthesis , characterization and reduction of graphene oxide: a convenient method for large scale production," *Egypt*, J. Basic Appl. Sci. 4 (1) (2017) 74–79, https://doi.org/10.1016/j.ejbas.2016.11.002.
[34] Q. Lai, S. Zhu, X. Luo, M. Zou, Shuanghua Huang, Ultraviolet-visible spectroscopy of grphene oxides, AIP 2 (32146) (2012) 5.
[35] J. Song, X. Wang, C. Chang, Preparation and characterization of graphene oxide, Hindawi 2014 (276143) (2014) 6, https://doi.org/10.1155/2014/276143.
[36] D. Khalili, "Graphene oxide: a promising carbocatalyst for the regioselective thiocyanation of aromatic amines , phenols , anisols and enolizable ketones by hydrogen peroxide/KSCN in water, New J. Chem. (2016) 1–11.
[37] S.I. Javed, Z. Hussain, "Covalently functionalized graphene oxide – characterization and its electrochemical performance, Int. J. Electrochem. Sci. 10 (2015) 9475–9487.
[38] P.T. Nam, et al., "Synthesis of reduced graphene oxide for high-performance supercapacitor, Vietnam J. Chem. 56 (6) (2018) 778–785, https://doi.org/10.1002/vjch.201800087.
[39] V.H. Pham, et al., Chemical functionalization of graphene sheets by solvothermal reduction of a graphene oxide suspension in Nmethyl- 2-pyrrolidone, J. Mater. Chem. 21 (2011) 3371–3377.
[40] S. Eigler, C. Dotzer, A. Hirsch, M. Enzelberger, P. Müller, Formation and decomposition of CO2 intercalated graphene oxide, Chem. Mater. 24 (7) (2012) 1276–1282.

[41] J. Huang, et al., Biosynthesis of silver and gold nanoparticles by novel sundried cinnamomum camphora leaf, Nanotechnology 18 (10) (2007) 105104–105115.
[42] M. Sohail, et al., "Modified and improved Hummer's synthesis of graphene oxide for capacitors applications, Mod. Electron. Mater. 3 (3) (2017) 110–116, https://doi.org/10.1016/j.moem.2017.07.002.
[43] S. Bykkam, V.R.K., S.C. Ch, T. Thunugunta, Synthesis and characterization of graphene oxide and its antimicrobial activity against klebseilla and staphylococus, Inter J. Adv. Biotechnol. Res. J. Adv. Biotechnol. Res. 4 (1) (2013) 142–146.
[44] N.I. Zaaba, K.L. Foo, U. Hashim, S.J. Tan, W. Liu, C.H. Voon, "Synthesis of graphene oxide using modified hummers method: solvent influence, Procedia Eng. 184 (2017) 469–477, https://doi.org/10.1016/j.proeng.2017.04.118.
[45] X. Shen, X. Lin, N. Yousefi, J. Jia, J.-K. Kim, Wrinkling in graphene sheets and graphene oxide papers, Carbon N. Y. 66 (2014) 84–92.
[46] R.I. Jibrael, M.K.A. Mohammed, Production of graphene powder by electrochemical exfoliation of graphite electrodes immersed in aqueous solution, Optik 127 (2016) 6384–6389.
[47] K. Zhou, Y. Zhu, X. Yang, X. Jiang, C. Li, Preparation of graphene-TiO2 composites with enhanced photocatalytic activity, New J. Chem. 35 (2) (2011) 353–359.
[48] J. Shen, M. Shi, B. Yan, H. Ma, N. Li, M. Ye, Ionic liquidassisted one-step hydrothermal synthesis of TiO2-reduced graphene oxide composites, Nano Res. 4 (8) (2011) 795–806.
[49] R.I. Jibrael, et al., Graphene-based polymer nanocomposites, Carbon N. Y. 6 (1) (2015) 1–4, https://doi.org/10.4172/2157-7439.1000253.
[50] S. Drewniak, R. Muzyka, A. Stolarczyk, T. Pustelny, M. Kotyczka-Moranska, M. Setkiewicz, Studies of reduced graphene oxide and graphite oxide in the aspect of their possible application in gas sensors, Sensors MDPI 16 (103) (2016) 16.
[51] S. Perumbilavil, P. Sankar, P.R. Thankamani, R. Philip, "White light Z-scan measurements of ultrafast optical nonlinearity in reduced graphene oxide nanosheets in the 400 – 700 nm region, Appl. Phys. Lett. 107 (51104) (2015) 7, https://doi.org/10.1063/1.4928124.
[52] K. Krishnamoorthy, M. Veerapandian, K. Yun, S.J. Kim, The chemical and structural analysis of graphene oxide with different degrees of oxidation, Carbon N. Y. 53 (2013) 38–49, https://doi.org/10.1016/j.carbon.2012.10.013.
[53] R. Gao, et al., Paper-like graphene-Ag composite films with enhanced mechanical and electrical properties, Nanoscale Res. Lett. 8 (32) (2013) 2–9 [Online]. Available, http://www.nanoscalereslett.com/content/8/1/32.
[54] J. Xie, P. Yang, Y. Wang, T. Qi, Y. Lei, C.M. Li, Puzzles and confusions in supercapacitor and battery_ Theory and solutions, J. Power Sources 401 (2018) 213–223, https://doi.org/10.1016/j.jpowsour.2018.08.090.
[55] A. Laheäär, P. Przygocki, Q. Abbas, F. Béguin, Appropriate methods for evaluating the ef fi ciency and capacitive behavior of different types of supercapacitors, Electrochem. Commun. 60 (2015) 21–25, https://doi.org/10.1016/j.elecom.2015.07.022.
[56] A. Allagui, et al., Review of fractional-order electrical characterization of supercapacitors _ Elsevier Enhanced Reader.pdf, J. Power Sources 400 (2018) 457–467, https://doi.org/10.1016/j.jpowsor.2018.08.047.
[57] L. Lai, et al., Preparation of supercapacitor electrodes through selection of graphene surface functionalities, ACS Nano 6 (2012) 5941–5951.
[58] L.T. Le, M.H. Ervin, H. Qiu, B.E. Fuchs, W.Y. Lee, Graphene supercapacitor electrodes fabricated by inkjet printing and thermal reduction of graphene oxide, Electrochem. Commun. 13 (2011) 355–358, https://doi.org/10.1016/j.elecom.2011.01.023.
[59] F.Y. Ban, S.R. Majid, N.M. Huang, H.N. Lim, Graphene oxide and its electrochemical performance, Int. J. Electrochem. Sci. 7 (2012) 4345–4351.
[60] C.-T. Hsieh, S.-M. Hsu, J.-Y. Lin, H. Teng, Electrochemical capacitors based on graphene oxide sheets using different aqueous electrolytes, J. Phys. Chem. C 115 (25) (2011) 12367–12374.
[61] T.S. Mathis, N. Kurra, X. Wang, D. Pinto, P. Simon, "Energy storage data reporting in perspective — guidelines for interpreting the performance of electrochemical energy storage systems, Adv. energy Mater. 1902007 (2019) 1–13, https://doi.org/10.1002/aenm.201902007.
[62] U. Saha, R. Jaiswal, T.H. Goswami, A facile bulk production of processable partially reduced graphene oxide as superior supercapacitor electrode material, Electrochim. Acta 196 (2016) 386–404.
[63] P.W. Ruch, D. Cericola, R. Kötz, A. Wokaun, Aging of electrochemical double layer capacitors with acetonitrile-based electrolyte at elevated voltages, Electrochim. Acta 55 (15) (2010) 4412–4420, https://doi.org/10.1016/j.electacta.2010.02.064.
[64] D. Weingarth, A. Foelske-Schmitz, R. Kötz, "Cycle versus voltage hold e Which is the better stability test for electrochemical double layer capacitors? J. Power Sources 225 (2013) 84–88, https://doi.org/10.1016/j.jpowsour.2012.10.019.